Earth and Planetary Science Letters 498 (2018) 17–26

Contents lists available at ScienceDirect

Earth and Planetary Science Letters

www.elsevier.com/locate/epsl

Temperate ice in the shear margins of the Antarctic Ice Sheet: Controlling processes and preliminary locations

Colin R. Meyer [a,*], Brent M. Minchew [b]

[a] Department of Earth Sciences, University of Oregon, Eugene, OR, 94703, USA
[b] Department of Earth, Atmospheric & Planetary Sciences, Massachusetts Institute of Technology, Cambridge, MA, 02139 USA

ARTICLE INFO

Article history:
Received 6 April 2018
Received in revised form 9 May 2018
Accepted 13 June 2018
Available online xxxx
Editor: B. Buffett

Keywords:
temperate ice
shear margins
ice streams
ice flow
deformation heating
glacier thermomechanics

ABSTRACT

The flux of grounded ice from the Antarctic Ice Sheet (AIS) primarily occurs through narrow, fast-flowing outlet glaciers and ice streams. Shearing generates heat in the lateral glacier margins, where there is a transition from fast-flow to near-stagnant ice or rock. This heat warms the ice and can form zones of water-saturated porous ice at the melting temperature, known as temperate ice. Here we derive a one-dimensional thermomechanical model to infer which AIS shear margins may contain temperate ice. Our model provides expressions for the critical shear strain rate at which a zone of temperate ice initiates and the thickness of the temperate zone. Both of these quantities are described by two nondimensional numbers—the Brinkman and Péclet numbers—that are functions of observable parameters such as shear strain rate, surface temperature, surface accumulation rate, and ice thickness. The development of temperate zones is incited by shear strain rates (Brinkman number) and suppressed by the advection of cold ice from the surface (Péclet number), which scales with surface accumulation rate. We also include a parametrization for lateral advection, which can suppress the formation of temperate ice. Applying recent observations and outputs from a regional climate model, we show that many active glacier shear margins could contain temperate ice. The spatial distribution and thickness of temperate zones are controlled largely by shear strain rates and surface accumulation rates.

1. Introduction

Outlet glaciers and ice streams in Antarctica transport the majority of the grounded ice to the ocean (Rignot et al., 2011). Regions of fast flow are driven by gravity and resisted by basal drag and lateral shear at the margins (Echelmeyer et al., 1994; Kamb, 2001). The partitioning of drag between the shear margins and the bed varies across Antarctica. In some cases, weak basal sediments underlying fast-flowing regions cause the basal shear stress to be a small component of the force balance, requiring the majority of the driving stress to be accommodated by lateral shear in the margins (Raymond, 1996; Tulaczyk et al., 2000; Joughin et al., 2004). Ice shelves provide further resistance to glacier flow through lateral shear in their margins and drag at basal pinning points.

Shear margins in Antarctica exist on ice shelves with negligible basal shear stress, outlet glaciers that flow through mountain valleys, and ice streams that are not topographically controlled. The transition from fast to slow flow in the margins facilitates the dissipation of energy by friction, which increases the ice temperature. The temperature of glacier ice controls the rate at which it flows by modulating the ice viscosity. From the typical surface temperatures in Antarctica to the melting temperature, the ice viscosity softens by an order of magnitude (Cuffey and Paterson, 2010). Thus, within shear margins there is the potential for a thermoviscous feedback where shearing generates heat, which softens the ice allowing for more shearing (Clarke et al., 1977; Hindmarsh, 2004, 2009). This thermal-runaway mechanism can be used to model the formation of ice streams (Fowler and Johnson, 1996; Kyrke-Smith et al., 2013; Schoof and Hewitt, 2013).

Models suggest that deformation in ice stream shear margins can generate enough heat to form temperate ice, a mechanically strong mixture of porous ice and liquid water that is at the melting temperature. An idealized model for a shear margin is an abrupt transition from free-slip to no-slip conditions at the ice–bed interface (Perol et al., 2015; Meyer et al., 2016, 2017). Using this model, Jacobson and Raymond (1998) and Suckale et al. (2014) numerically, and Schoof (2004, 2012) analytically solve for the temperature in a shear margin and show the development of temperate ice. Using observed shear strain rates to compute the deformation heat in a one-dimensional numerical model, which excludes lateral and downstream advection, Perol and Rice (2011, 2015) find

* Corresponding author.
E-mail address: colinrmeyer@gmail.com (C.R. Meyer).

https://doi.org/10.1016/j.epsl.2018.06.028
0012-821X/

temperate ice in all active Siple Coast shear margins. Suckale et al. (2014) study the effects of across-stream lateral advection of cold ice on temperate zone development. This lateral advection can arise either as ice flow from the adjoining ridges or by lateral migration of the shear margin (Schoof, 2004; Echelmeyer and Harrison, 1999; Haseloff et al., 2015). Suckale et al. (2014) find that sufficiently high rates of lateral advection can extinguish a temperate zone and, also conclude that a temperate zone is necessary to explain the observed shear strain rates, indicating that there cannot be significant across-stream advection (or margin migration) in their study area.

In this paper, we present a study of deformation heating in lateral shear margins across the Antarctic Ice Sheet. We derive a one-dimensional, analytical thermomechanical model with a focus on understanding the prevalence and thickness of shear-induced temperate ice. We include lateral advection and show how it will affect our results. Our model is analytical, which means that it can be readily interpreted and used as a guide for more detailed studies in the future. The model provides a prediction for the critical shear strain rate at which temperate ice develops and an estimate of the thickness of the temperate zone. Using shear strain rate fields calculated from recent observations of surface velocity, we infer the possible locations and thicknesses of zones of temperate ice in the shear margins in the Antarctic Ice Sheet.

2. Model development

As ice deforms, heat is generated that warms cold ice and melts temperate ice. In this section, we describe a one-dimensional model for the temperature distribution within a column of ice that includes advection, conduction, and deformation-induced internal heating. We build on the ideas of Perol and Rice (2011, 2015) and follow Schoof and Hewitt (2016) in explicitly deriving a thermomechanical model that can be combined with a suite of observations to determine the effects of shear heating. Our goal is to develop a model that captures the salient physics yet is simple enough to be easily implemented and applied broadly.

To illustrate the fundamental concepts, we derive the model in two steps beginning with the simplest relevant model, in which we neglect advection, followed by the more generalized form that we use for our results, in which we include lateral and vertical advection. Further details are provided in the supplement, where we also explore the consequences of the assumptions and simplifications in our model.

2.1. Diffusion solution

We consider a coordinate system where x is the downstream direction, y is the across flow coordinate, and z is vertical within the ice such that $z = 0$ at the bed and $z = H$ at the surface. In this first model, we ignore vertical and lateral advection. Therefore, conservation of energy implies that the steady state temperature T within the ice column is given by

$$K\frac{d^2T}{dz^2} = -\sigma_{ij}\dot{\epsilon}_{ij}, \tag{1}$$

where K is the thermal conductivity, assumed constant, and we use the summation convention for repeated indices. Table 1 contains the values for the parameters. In Equation (1), $\sigma_{ij}\dot{\epsilon}_{ij}$ is the rate of deformation heating, wherein σ_{ij} is the Cauchy stress tensor and $\dot{\epsilon}_{ij}$ is the strain rate tensor. Stress and strain rate are related through the rheology of ice, which is given by Glen's law as

$$\sigma_{ij} = -p\delta_{ij} + A^{-1/n}\left(\frac{1}{2}\dot{\epsilon}_{kl}\dot{\epsilon}_{kl}\right)^{(1-n)/(2n)}\dot{\epsilon}_{ij}, \tag{2}$$

Table 1
Parameters for the thermomechanical model.

ρ	917 $\mathrm{kg\,m^{-3}}$
c_p	2050 $\mathrm{J\,kg^{-1}\,K^{-1}}$
T_m	273 K
K	2.1 $\mathrm{W\,m^{-1}\,K^{-1}}$
A	2.4×10^{-24} $\mathrm{Pa^{-3}\,s^{-1}}$
n	3

where p is the pressure, δ_{ij} is the Kronecker delta, A is the temperature-dependent ice softness, and the exponent is typically $n \approx 3$ (Cuffey and Paterson, 2010).

Applying Glen's law, we can approximate the rate of deformation heating as

$$\sigma_{ij}\dot{\epsilon}_{ij} \approx 2A^{-1/n}\dot{\epsilon}_{\mathrm{lat}}^{(n+1)/n}, \tag{3}$$

in areas, such as the shear margins of glaciers and ice streams, where the dominant component of the strain rate tensor is the nonnegative lateral shear strain rate $\dot{\epsilon}_{\mathrm{lat}}$. This strain rate arises due to lateral variation in the downstream ice-flow velocity u, *i.e.* $\dot{\epsilon}_{\mathrm{lat}} = |\dot{\epsilon}_{xy}| = |\partial u/\partial y|/2$. As written, Equation (1) could lead to ice temperatures in excess of the melting point T_m (Perol and Rice, 2011, 2015), and we avoid this nonphysical condition by imposing $T \leq T_m$ through the boundary conditions.

To solve Eq. (1) for depth-dependent temperature, we impose three boundary conditions. The first two conditions apply to ice temperature such that

$$T = T_m \qquad \text{at} \qquad z = \xi, \tag{4a}$$

$$T = T_s \qquad \text{at} \qquad z = H, \tag{4b}$$

where T_s is the ice surface temperature, T_m is the melting temperature of ice, and we allow for the possibility of a temperate zone (a region where $T = T_m$) that extends from the bed to $z = \xi$ (Fig. 1(a)). The third boundary condition applies to the heat flux and serves two important purposes: it enforces $T \leq T_m$ everywhere in the domain by preventing heat flux across the cold-temperate boundary at $z = \xi$, and allows us to determine ξ, the thickness of the temperate zone. This boundary condition, defined as

$$-K\frac{\partial T}{\partial z} = 0 \qquad \text{at} \qquad z = \xi, \tag{5}$$

enforces conservation of energy across the boundary between cold and temperate ice (Hutter, 1983; Worster, 2000; Hewitt and Schoof, 2017).

The formulation in Equations (1)–(5) is known as a contact or obstacle problem where the melting temperature is the barrier (Johnson, 1987; Howell et al., 2008; Schoof and Hewitt, 2016). This description provides some intuition by allowing us to visualize the problem of determining the temperate zone thickness ξ as analogous to finding the contact radius of a deformable soccer ball as it is pressed against a table. In this analogy, the soccer ball represents ice temperature and the table is the melting temperature; just as the soccer ball cannot penetrate the table, the temperature of the ice cannot exceed the melting point. If we imagine initially holding the soccer ball below the table (cold ice) and then moving it upward (warming the ice), once the soccer ball (ice temperature) reaches the table (melting point), any additional pressure (heat) causes the radius of contact between the ball and table (temperate zone) to grow.

In order to derive an analytical solution for the steady state temperate-ice-zone thickness ξ, we take deformation heating to be independent of depth and neglect the pressure-dependence of T_m.

Integrating Equation (1) subject to the boundary conditions in (4) and (5), we find that

$$T = \begin{cases} T_s + \Delta T \dfrac{\mathrm{Br}}{2}\left[1 - \left(\dfrac{z}{H}\right)^2 - 2\dfrac{\xi}{H}\left(1 - \dfrac{z}{H}\right)\right], & \xi \le z \le H \\ T_m, & 0 \le z < \xi \end{cases} \tag{6}$$

where the temperature difference is $\Delta T = T_m - T_s$ and the Brinkman number $\mathtt{Br}$ is the nonnegative, dimensionless ratio of deformation heating to thermal conduction given as

$$\mathtt{Br} = \frac{\sigma_{ij}\dot{\epsilon}_{ij}H^2}{K\Delta T} \tag{7a}$$

$$\approx \frac{2H^2}{K\Delta T}\left(\frac{\dot{\epsilon}_{\mathrm{lat}}^{n+1}}{A}\right)^{1/n} \tag{7b}$$

where we apply Equation (3) in Equation (7b). Increasing the Brinkman number can lead to the formation of temperate ice because the rate of deformation-induced heating exceeds the rate of heat conduction.

Whenever $T_s < T_m$, there is a nonzero critical shear strain rate $\dot{\epsilon}_{\mathrm{lat}}^{*}$ that will cause a zone of temperate ice to form. Recalling that $T = T_m$ at $z = \xi$, we plug Equation (3) into Equation (6) and solve for the critical shear strain rate $\dot{\epsilon}_{\mathrm{lat}}^{*}$ where temperate ice initiates, i.e. when $\xi = 0$. This gives

$$\dot{\epsilon}_{\mathrm{lat}}^{*} = \left(\frac{K\Delta T}{A^{-1/n}H^2}\right)^{n/(n+1)}. \tag{8}$$

Then, rearranging Equation (6) with $T = T_m$ at $z = \xi$, we find the thickness of a temperate zone induced by strain rates exceeding the critical strain rate as

$$\frac{\xi}{H} = \begin{cases} 1 - \sqrt{\dfrac{2}{\mathtt{Br}}}, & \dot{\epsilon}_{\mathrm{lat}} > \dot{\epsilon}_{\mathrm{lat}}^{*} \\ 0, & \dot{\epsilon}_{\mathrm{lat}} \le \dot{\epsilon}_{\mathrm{lat}}^{*} \end{cases} \tag{9}$$

Equations (8) and (9) provide an intuitive foundation for understanding shear-induced melting of glacier ice. Importantly, Equation (8) indicates the rate at which we need to deform ice with thickness H and surface temperature T_s—two parameters that vary spatially over an ice sheet and can be determined from data—in order to induce melting. The numerator in Equation (8) represents the rate of heat conduction from the source. Higher thermal conduction necessitates higher strain rates to melt the ice. Conversely, thicker ice (larger H) requires lower shear strain rates in order to induce melting because the thick ice insulates the lower ice from the cold surface temperatures. Stiffer ice (smaller A) generates more heat for a given deformation rate (Equation (3)), thereby requiring lower shear strain rates to induce melting. Equation (9) indicates that in areas where strain rates exceed the critical strain rate and advection of cold ice is negligible, the thickness of the temperate zone is governed by the inverse square root of the Brinkman number.

2.2. Advection–diffusion solution

Neglecting vertical advection is unrealistic over much of Antarctica, where snow accumulates at the surface and is advected down through the ice column, carrying with it the cold surface temperatures. Moreover, in some Antarctic ice streams, cold ice can advect across the shear margins from the surrounding ridges. Intuitively, we should expect increasing rates of lateral and vertical advection to reduce the potential for temperate ice to form or to diminish the thickness of a temperate zone. Therefore, we include advection in Equation (1) and rederive the expressions for ξ and $\dot{\epsilon}_{\mathrm{lat}}^{*}$. We provide details for this more complex model in supplemental materials, and we summarize the salient points here.

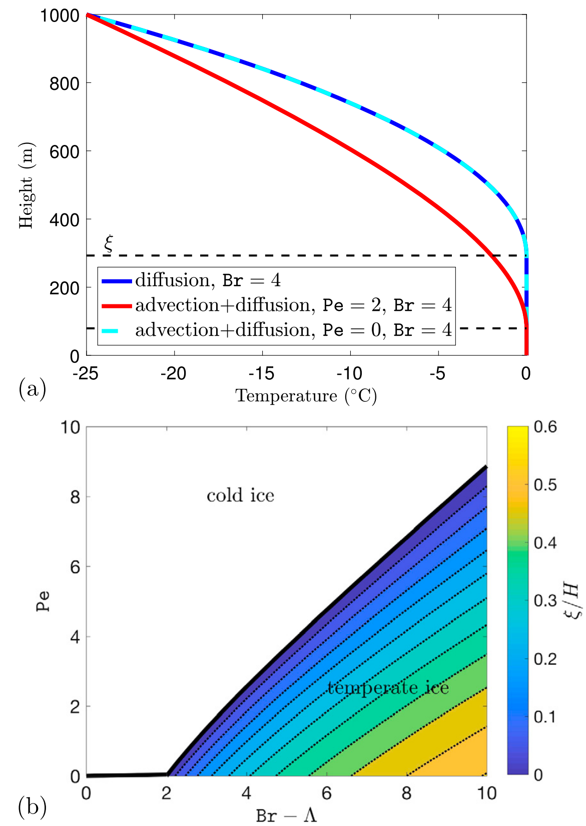

Fig. 1. Model for temperate zones within an ice column of $H = 1$ km and surface temperature $T_s = -25\,^{\circ}$C: (a) temperature as a function of height, comparing analytical solutions (6) and (13) without lateral advection ($\Lambda = 0$). (b) Relative thickness of the temperate zone ξ/H for a given Brinkman number $\mathtt{Br}$ less the lateral advection parameter Λ and vertical Péclet number $\mathtt{Pe}$ (colormap). The thick, black line shows $\mathtt{Br}$ required to form temperate ice for a given $\mathtt{Pe}$ and dotted contour lines delineate constant values of ξ/H (color online).

We start by including vertical and lateral advection as well as diffusion in the equation for conservation of energy:

$$\rho c_p v \frac{\partial T}{\partial y} + \rho c_p w \frac{\partial T}{\partial z} = K\frac{\partial^2 T}{\partial z^2} + \sigma_{ij}\dot{\epsilon}_{ij}, \tag{10}$$

where ρ is the density and c_p is the specific heat capacity of ice. To retain the simple, analytically tractable nature of our model while accounting for the vertical advection of cold ice from the surface, we take the vertical velocity w to be $w = -a$, where a is the surface mass balance ($a > 0$ for accumulation). We justify using a depth-independent vertical velocity for two reasons. Firstly, the simplicity of this solution allows us to write an analytical expression that we can apply to the entire ice sheet. Secondly, downward vertical advection diminishes the temperate zone thickness (viz. Fig. 1). A more natural expression for downward advection would include depth dependence and would vary from a maximum value at the surface to zero at the bed, thereby reducing the rate of vertical advection of cold ice in the deeper, warmer zone. A depth-independent vertical velocity results in a higher rate of vertical advection into the warmer ice at depth, which diminishes the thickness of the temperate zone. Holding all other variables constant, a depth-independent vertical advection provides a lower bound on the thickness of the temperate zone. This assumption is discussed in more detail in the supplement.

We consider the influence of lateral advection by defining the depth-averaged lateral advection term $\bar{\lambda}$ such that

$$\bar{\lambda} = \frac{\rho c_p}{H} \int_0^H v \frac{\partial T}{\partial y} \mathrm{d}z. \tag{11}$$

This term enters Equation (10) as a constant, allowing for scaling analysis. As we show in the results, shear strain rates are $\sim$0.1 yr^{-1} in most of the shear margins of interest. Scaling the ice softness as $A \sim 10^{-24}$ Pa^{-3} s^{-1}, approximately the maximum value given by Cuffey and Paterson (2010), Equation (3) gives the rate of shear heating $\sigma_{ij}\dot{\epsilon}_{ij} \sim 10^{-3}$ W/m^3. From Equation (11) with $v \sim 1$ m/yr and $\partial T/\partial y \sim 10^{-3}$ K/m (Suckale et al., 2014), we have $\sigma_{ij}\dot{\epsilon}_{ij}/\bar{\lambda} \sim 100$. Thus, in many areas of Antarctica with high shear strain rates, lateral advection can be neglected without incurring significant errors. Furthermore, while it may be desirable to include the effects of lateral advection in some areas due to inflow from the ridge or outward margin migration, lateral advection rates into shear margins are uncertain and cannot be resolved in available surface velocity observations due to observational errors and limitations in spatial resolution (Mouginot et al., 2017; Gardner et al., 2018). Even where rates of across-stream advection may be well-constrained (Harrison et al., 1998; Echelmeyer and Harrison, 1999), the net effect of lateral advection remains unclear. As previously noted, detailed model studies have shown that across-stream advection can diminish a temperate zone, but that the resulting colder, stiffer ice fails to explain the observed shear strain rates (Suckale et al., 2014). Indeed, close agreement was found between a two-dimensional model that includes across-stream lateral advection and a one-dimensional model that neglects lateral advection (see Suckale et al., 2014, Fig. 7). We therefore neglect lateral advection in the remainder of this study (i.e. take $\bar{\lambda} \ll \sigma_{ij}\dot{\epsilon}_{ij}$ everywhere) and consider our model results to be a reasonable first inference of the spatial distribution and potential thickness of temperate zones across most of the Antarctic Ice Sheet. For the rest of the model section, we include lateral advection $\bar{\lambda}$ to show how lateral advection could affect the development of a zone of temperate ice and to aid in our discussion.

With these assumptions, the energy balance becomes

$$-\rho c_p a \frac{\partial T}{\partial z} = K \frac{\partial^2 T}{\partial z^2} + \sigma_{ij}\dot{\epsilon}_{ij} - \bar{\lambda}. \tag{12}$$

In the supplement, we solve this equation for temperature subject to the boundary conditions given in Equations (4) and (5) and find that

$$T = \begin{cases} T_s + \Delta T \dfrac{\mathtt{Br} - \Lambda}{\mathtt{Pe}} \left[1 - \dfrac{z}{H} + \dfrac{1}{\mathtt{Pe}} \exp\left\{ \mathtt{Pe} \left(\dfrac{\xi}{H} - 1 \right) \right\} \right. \\ \qquad \left. - \dfrac{1}{\mathtt{Pe}} \exp\left\{ \mathtt{Pe} \left(\dfrac{\xi - z}{H} \right) \right\} \right], \quad \xi \le z \le H \\ T_m, \quad 0 \le z < \xi \end{cases} \tag{13}$$

which shows that the temperature T profile is now governed by three dimensionless numbers. The first is the aforementioned Brinkman number $\mathtt{Br}$ (Equation (7a)). The second dimensionless number is the vertical Péclet number $\mathtt{Pe}$, which is the ratio of accumulation to diffusion defined as

$$\mathtt{Pe} = \frac{\rho c_p a H}{K}. \tag{14}$$

The third is the lateral advection parameter

$$\Lambda = \frac{\bar{\lambda} H^2}{K \Delta T}, \tag{15}$$

which is the horizontal Péclet number, though we do not use this moniker to avoid confusion with the vertical Péclet number $\mathtt{Pe}$. Using these dimensionless quantities, we find the critical strain rate for temperate ice formation to be

$$\dot{\epsilon}^*_{\mathrm{lat}} = \left(\frac{\frac{1}{2}\mathtt{Pe}^2}{\mathtt{Pe} - 1 + \exp\{-\mathtt{Pe}\}} + \frac{1}{2}\Lambda \right)^{n/(n+1)} \left[\frac{K \Delta T}{A^{-1/n} H^2} \right]^{n/(n+1)}, \tag{16}$$

which simplifies to Equation (8) as $\mathtt{Pe}$ and Λ vanish. Comparing Equation (16) with (8) shows that the shear strain rate required to form temperate ice increases with the rate of lateral and vertical advection (Fig. 1). The thickness of the temperate zone ξ can be determined from the solution of Equation (12) in terms of the Lambert-W function as

$$\frac{\xi}{H} = \begin{cases} 1 - \dfrac{\mathtt{Pe}}{\mathtt{Br} - \Lambda} \\ \quad - \dfrac{1}{\mathtt{Pe}} \left[1 + \mathrm{W} \left(- \exp\left\{ - \dfrac{\mathtt{Pe}^2}{\mathtt{Br} - \Lambda} - 1 \right\} \right) \right], \quad \dot{\epsilon}_{\mathrm{lat}} > \dot{\epsilon}^*_{\mathrm{lat}} \\ 0, \quad \dot{\epsilon}_{\mathrm{lat}} \le \dot{\epsilon}^*_{\mathrm{lat}} \end{cases} \tag{17}$$

which simplifies to Equation (9) as $\mathtt{Pe}$ and Λ vanish.

Lambert-W, also known as the product logarithm, is the inverse function of $f(\mathrm{W}) = \mathrm{W}e^{\mathrm{W}}$ and is a built-in function in MATLAB, SciPy, Mathematica, and other scientific computational libraries. Lambert-W has multiple branches and is defined in the complex plane. For our purposes, we can restrict our usage to the primary, real-valued branch of $\mathrm{W}(\psi)$ because the argument, $\psi(\mathtt{Pe}, \mathtt{Br}, \Lambda)$, in Equation (17) is real-valued and $-e^{-1} < \psi < 0$. These conditions ensure that $\mathrm{W}(\psi)$ is real-valued and $-1 < \mathrm{W}(\psi) < 0$ whenever $\dot{\epsilon}_{lat} > \dot{\epsilon}^*_{lat}$. Furthermore, $\mathrm{W}(\psi) \to -1$ as $\psi \to -e^{-1}$ (and $\mathrm{W}(\psi) \to \psi$ as $\psi \to 0$), meaning that larger (smaller) Brinkman numbers, for given values of $\mathtt{Pe}$ and Λ, cause the bracketed term in Equation (17) to tend toward zero (unity). The influence of W on the thickness of the temperate zone is shown in Fig. 1(b), where the contour lines that trace constant values of ξ/H are slightly concave, owing to the influence of the final term in Equation (17).

We also note that ice softness A can be a function of ice crystalline orientation, commonly known as fabric. The influence of fabric on the ice rheology can be parameterized with an enhancement factor E such that $A = EA_b$ and A_b is the background ice softness (Cuffey and Paterson, 2010). Including an enhancement factor in Equation (16) increases the minimum strain rate by a factor of $E^{1/(n+1)}$ or about 1.8 for $E = 10$, the approximate upper limit of fabric enhancement based on laboratory measurements (Jacka and Budd, 1989; Jackson and Kamb, 1997). Therefore, fabric, by softening the ice and decreasing the rate of deformation heating, could increase $\dot{\epsilon}^*_{\mathrm{lat}}$ by no more than a factor of 2. In calculating $\dot{\epsilon}^*_{\mathrm{lat}}$ and ξ for modern conditions in Antarctica, we implicitly account for fabric by taking A to be the value for temperate ice given by Cuffey and Paterson (2010), which is approximately 40 times greater than the value given by the same authors for ice at $-25\,°$C. This value for A is a reasonable choice because the only locations where its value will be important in our analysis is in a temperate zone. Moreover, Equations (9) and (17) show that the temperate zone cannot extend over the entire ice thickness, making this an overestimate of the ice softness that will diminish the predicted thickness of the temperate zone. For this reason and our assumption of depth-independent vertical advection, our model gives the lower bound for temperate-zone thickness as long as lateral and downstream advection are negligible.

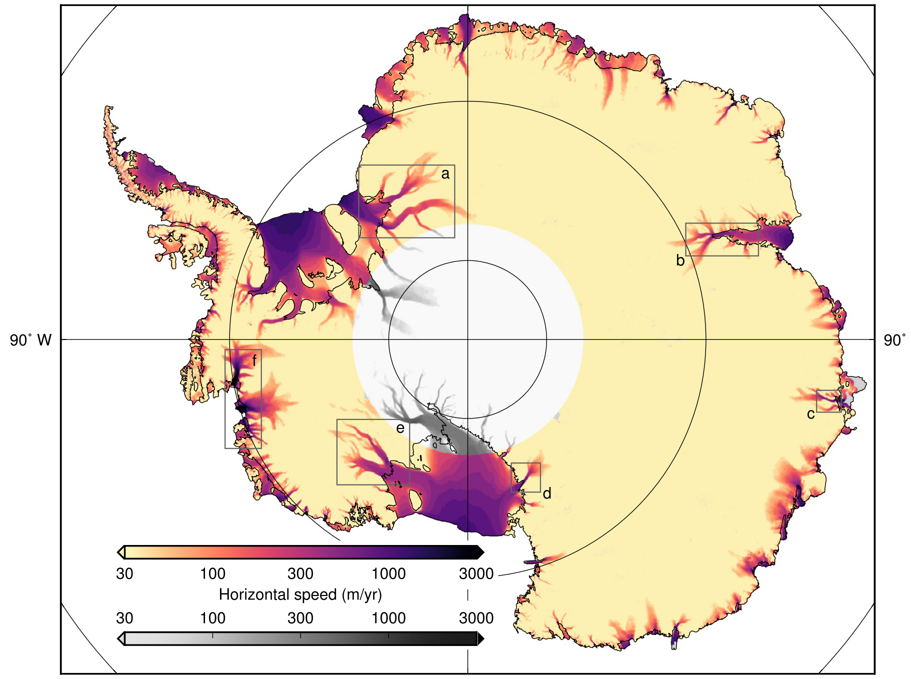

Fig. 2. Observed surface velocities for the Antarctic Ice Sheet. Values in color are derived from Landsat 7 and 8 satellite imagery acquired from 2014 to 2015 (Gardner et al., 2018) and values in grayscale, which are not used in this study and are provided only for context, are from synthetic aperture radar data (Rignot et al., 2011; Mouginot et al., 2012, 2017). Sinuous black lines indicate the grounding lines given by Fretwell et al. (2013). The regions of interest (ROI) for this study are outlined by the gray rectangles. The ROI letters are the same in Figs. 2–5, and the major glaciers and ice streams in each are: (a) Slessor and Recovery Glaciers; (b) Mellor and Lambert Glaciers; (c) Denman Glacier; (d) Byrd Glacier; (e) Bindschadler and MacAyeal Ice Streams; and (f) part of the Amundsen Sea Embayment, including Pine Island, Thwaites, and Kohler Glaciers (color online).

3. Data and methods

We use recent, publicly available observations of surface velocity to calculate shear strain rate over most of Antarctica (Fig. 2). The surface velocity fields were derived from satellite imagery collected with Landsat 7 and Landsat 8 between 2014 and 2015 (Gardner et al., 2018). The data are provided with 240-m spatial resolution and standard errors of 30 m/yr. We use a second-order Savitzky–Golay filter with a ∼2.5-km square window to calculate the shear strain rate field (Fig. 4) from the surface velocity field (Fig. 2). The inclination of the satellite orbits limits the southern extent of the data coverage to approximately 82° S, creating a data hole in the center of the ice sheet. While data are available to complete the velocity map (grayscale in Fig. 2), the sparse data coverage south of 82° S results in velocity data in which the portions of the shear margins with high shear strain rates are insufficiently resolved for our purposes (Rignot et al., 2011; Mouginot et al., 2012, 2017).

In addition to surface velocity fields, our model requires inputs for surface mass balance and temperature as well as ice thickness, which are shown in Fig. 3. For surface mass balance and surface temperature, we average yearly results for 1979–2014 from RACMO2.3, provided on a 27-km grid (van Wessem et al., 2014), which does not include the effects of cold-air ponding in shear margin crevasses (Harrison et al., 1998). For ice thickness, we use Bedmap2 results, provided at 1-km grid spacing (Fretwell et al., 2013). We resampled all data fields to the same grid as the velocity fields using bi-linear interpolation.

4. Results and discussion

Zones of temperate ice can exist where the rate of heating exceeds both the rate of thermal conduction and the rates of vertical advection of cold ice from the surface and lateral advection of cold ice into the margins. Each of these factors are described in our model by dimensionless numbers that are functions of intrinsic material properties—such as density, specific heat capacity, and thermal conductivity—and observable, spatially varying parameters like shear strain rate, surface temperature, surface accumulation rate, and ice thickness. The Brinkman number, $\mathtt{Br}$, represents the rate of shear heating relative to thermal conduction and is driven by observed shear strain rates (Fig. 4). The vertical Péclet number, $\mathtt{Pe}$, accounts for the relative values of vertical advection and diffusion and is driven by the surface accumulation rate (Fig. 3a). The lateral advection parameter, Λ, indicates that the depth-averaged lateral advection effectively reduces the Brinkman number.

We explore the parameter space in Fig. 1, where we show temperature profile and the thickness of the temperate zone for different Péclet numbers, Brinkman numbers, and lateral advection parameters. High shear strain rates, i.e. larger Brinkman numbers, are required to overcome the downward vertical advection of cold ice from the surface in order to form temperate ice. Large Brinkman numbers are also required for temperate ice to form where there is significant lateral advection. Our model shows that lateral advection linearly reduces the size of the Brinkman number as $\mathtt{Br} - \Lambda$ (Equation (17)). Therefore, for a given $\mathtt{Pe}$, the effect of lateral advection on the thickness of the temperate zone thickness can be visualized by simply moving left along the abscissa in Fig. 1(b). The boundary between cold and temperate ice in the parameter space (heavy black line in Fig. 1b) shows that, to a good approximation, the condition for the development of a zone of temperate ice is met for any Péclet number that can be expected for Antarctica when $\mathtt{Br} - \Lambda > \mathtt{Pe} + 2$. Therefore, where $\Lambda \ll \mathtt{Br}$, which we assume to be the case for the remainder of this study, the $\mathtt{Br}/\mathtt{Pe}$ ratio provides insight into the thermomechanics of ice sheets and a convenient way to identify shear margins that may contain temperate ice (Fig. 5).

Our results indicate that many glaciers and ice streams in Antarctic Ice Sheet could contain zones of temperate ice in the shear margins. With the insets in Figs. 4 and 5, we highlight six re-

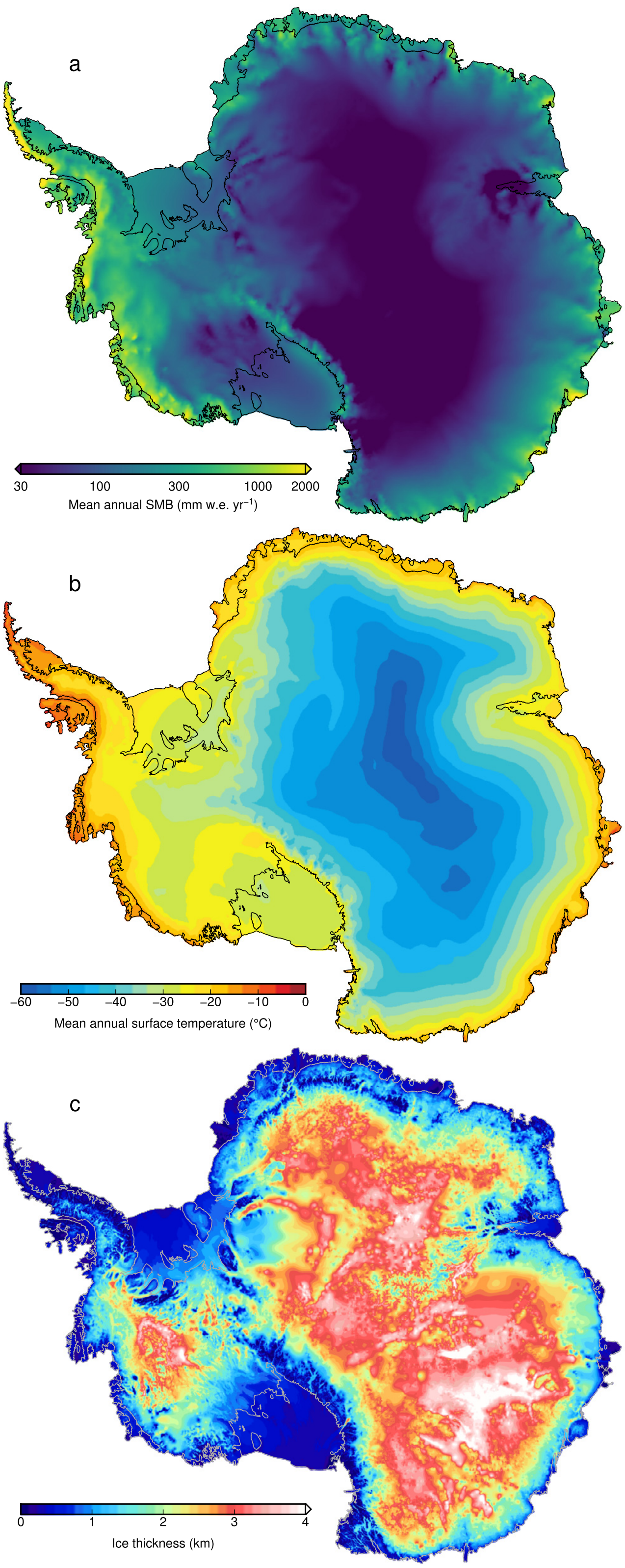

Fig. 3. Antarctic Ice Sheet (a) surface mass balance and (b) surface temperature from RACMO2.3 (van Wessem et al., 2014) along with (c) ice thickness from Bedmap2 (Fretwell et al., 2013). Grounding lines are the same as in Fig. 2 (color online).

gions with glaciers and ice streams that have observed shear strain rates well in excess of the local critical strain rate over significant distances. These glaciers and ice streams are located in the East Antarctic Ice Sheet (EAIS) and the West Antarctic Ice Sheet (WAIS), and may contain deformation-induced temperate-ice zones exceeding half of the local ice thickness (Fig. 5).

In EAIS, the outlet glaciers that our model indicates may contain significant temperate zones are Recovery and Slessor Glaciers; Lambert and Mellor Glaciers; Byrd Glacier; and Denman Glacier (Figs. 4 and 5, insets a–d, respectively). With the exception of Denman Glacier, the EAIS glaciers and ice streams with the potential to form temperate zones do not have exceptionally high shear strain rates (Fig. 4). Instead, the possible existence of temperate-ice zones is enabled by low surface accumulation rates, resulting in low rates of downward vertical advection of cold ice, i.e. low vertical Péclet numbers (Figs. 3 and S1). The average rate of downward vertical advection of cold ice over Denman Glacier, on the other hand, is more than three times higher than the other EAIS regions of interest. Yet the shear strain rates (Brinkman numbers) on Denman are sufficiently high that a temperate-ice zone likely exists.

In WAIS, some Siple Coast ice streams and some glaciers in the Amundsen Sea Embayment may have zones of deformation-induced temperate ice (Suckale et al., 2014; Perol and Rice, 2015; Elsworth and Suckale, 2016). Notably, many of the ice streams that drain into the Ronne Ice Shelf, such as Rutford Ice Stream, most likely do not contain temperate ice, which is consistent with the results of Minchew et al. (2018). Bindschadler Ice Stream (Figs. 4 and 5, inset e), on the Siple Coast, might contain several isolated zones of temperate ice within its complex system of margins. These are some of the thinnest predicted temperate zones in our areas of interest and are facilitated more by low rates of downward vertical advection of cold ice than by exceptionally high shear strain rates. The thickest part of the modeled temperate zone on Bindschadler rises to approximately half of the ice thickness and lies in the southern margin near the grounding line, in agreement with Elsworth and Suckale (2016). Temperate zones also likely exist on the Whillans Ice Stream as shown by Perol and Rice (2011, 2015) using a similar model to what we use in this paper. Although the velocity data from this region of WAIS are insufficiently resolved to be included in our study, the RACMO2.3 accumulation rates (Fig. 3(a)) and strain rates from Joughin et al. (2004) indicate that temperate ice is likely in the shear margins of Whillans and Mercer Ice Streams.

Glaciers in the Amundsen Sea Embayment (Figs. 4 and 5, inset f) stand out from the other regions of interest because they contain high surface accumulation and high shear strain rates. This characteristic is best represented on Pine Island Glacier, where some of the highest strain rates in the Antarctic Ice Sheet might be sufficient to overcome moderately high rates of downward vertical advection to produce temperate zones. In some places along the Pine Island shear margins, the predicted thickness of the temperate region exceeds three-quarters of the local ice thickness in both shear margins and on both the grounded glacier and the floating ice shelf. This prediction of an exceptionally thick temperate zone warrants further study and highlights the fact that our model can be used to select such regions of interest. Kohler Glacier may contain zones of temperate ice rising more than halfway up the ice column in both shear margins. These two temperate zones terminate where Smith Glacier intersects Kohler Glacier, suggesting that the observed shear strain rates reflect the stiffening of ice caused by the lateral advection of cold ice, and thus neglecting lateral advection may not contaminate our results (cf. Suckale et al., 2014). Finally, high accumulation rates prevent the development of temperate ice in the margins of Thwaites Glacier. The small region of temperate ice immediately upstream of the Thwaites grounding line is probably enabled by the lack of downstream or lateral advection in our model and is therefore unlikely to be a robust prediction.

In areas where our model predicts that outlet glacier shear margins contain thick zones of temperate ice immediately upstream of

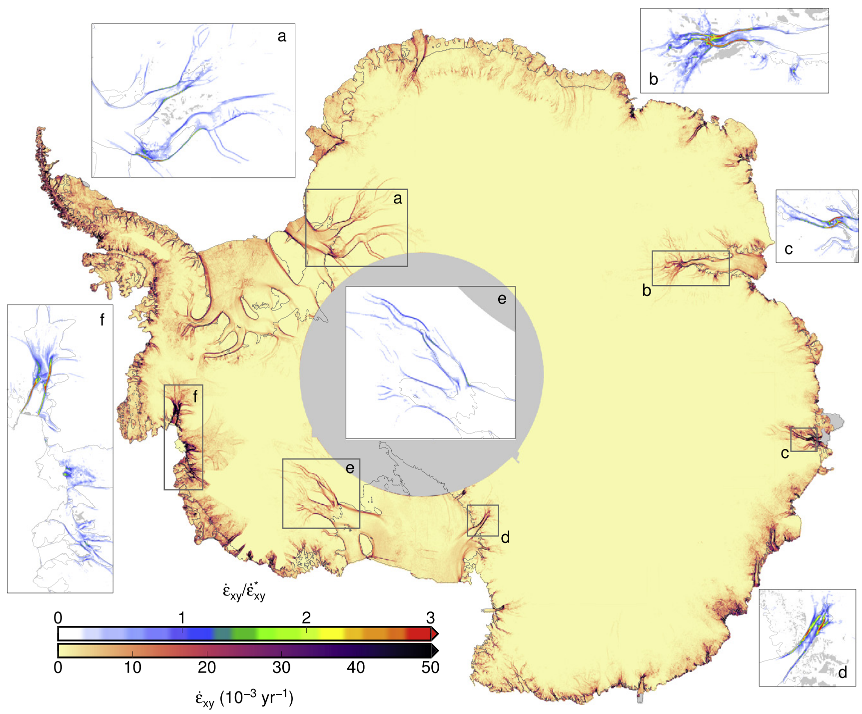

Fig. 4. Shear strain rates in the Antarctic Ice Sheet. The complete map shows shear strain rates calculated from the observed surface velocity fields (Fig. 2); gray lines indicate the grounding line from Fretwell et al. (2013). Insets show the ratio of observed shear strain rates to the critical strain rates (calculated from Equation (16)) in the regions of interest; gray lines are the 250 m/yr horizontal flow speed contours and black lines trace the grounding lines.

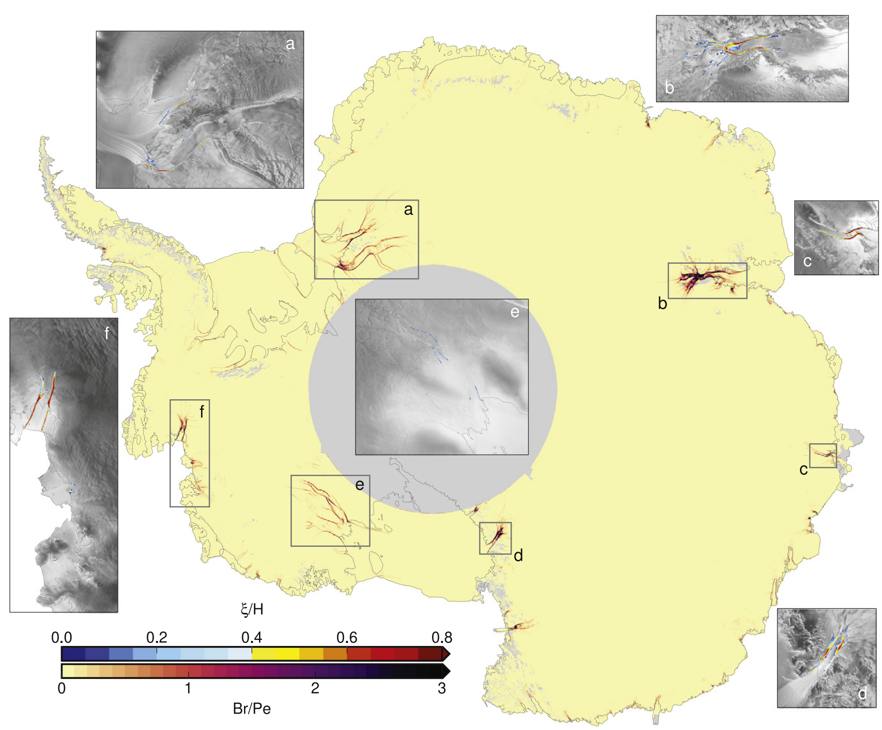

Fig. 5. Internal melting in the Antarctic Ice Sheet. The complete map shows the ratio of Brinkman number Br to vertical Péclet number Pe; gray lines indicate the grounding line from Fretwell et al. (2013). Insets show nonzero normalized temperate zone thickness (ξ/H) calculated from Equation (17) overlaying radar backscatter images from Jezek et al. (2013) with black lines tracing the grounding lines.

the grounding line, the floating ice shelves downstream contain shear margins, even where there is no obvious lateral confinement from the bed topography (Fig. 4). These ice shelf shear margins follow the flow trajectory across the grounding line and can extend more than 100 km downstream into the ice shelf. We hypothesize that the horizontal advection of softened, temperate ice from upstream of the grounding line, along with the development of surface and basal crevasses (Van der Veen, 1998), may allow for the existence of ice-shelf shear margins. The buttressing force that resists the downstream glacier motion would then depend on the rheology of ice in the ice-shelf shear margins. In this way, buttressing could also be susceptible to a thermoviscous feedback, wherein ice-shelf thinning due to a local increase in ocean temperature or enhanced transport of warm, deep water could result in faster ice flow, which would weaken the shelf shear margins, and further reduce ice-shelf buttressing. As a result, understanding the rheology of ice in ice-shelf shear margins is an important topic for future work.

Throughout the model development, we noted that our goal was to derive a simple, analytical model that captures the salient physical processes and provides a foundation to enhance our understanding of the thermomechanics of ice sheets. Our model, which is straightforward to implement and interpret, provides a unique look into the regions of temperate ice that may form in the shear margins of Antarctica. These benefits come at the expense of not including all possible physical processes. Three important limitations to our model are the lack of explicit treatment of mechanisms that might soften the ice (thereby reducing the rate of deformation heating), our use of a depth-independent vertical velocity, and our decision to use a one-dimensional vertical model, which prevents a full treatment of horizontal advection. As discussed in §2.2, the development of crystalline fabric can increase the critical strain rate necessary to produce temperate ice by up to a factor of 2. We implicitly account for the effects of fabric by prescribing the maximum value for ice softness A given by Cuffey and Paterson (2010, Table 3.4), which corresponds to temperate ice. This value for the ice softness is approximately 40 times greater than the value expected for ice at $-25\,^{\circ}\mathrm{C}$, a typical surface temperature in our areas of interest (Fig. 3(b)). As it is not possible for a temperate zone to extend to the full ice thickness, the value of A in all margins should be less than the value for temperate ice. Thus, our decision to use the value of A corresponding to temperate ice (cf. Cuffey and Paterson, 2010) is a conservative choice that causes our results to reflect the minimum value of deformation heating. Taking into account any softening of the ice that is not accounted for through our use of a temperate value for A, we note that our confidence in the existence of temperate ice increases with the ratio $\dot{\epsilon}_{\mathrm{lat}}/\dot{\epsilon}^*_{\mathrm{lat}}$. We consider the presence of temperate ice to be unlikely where $\dot{\epsilon}_{\mathrm{lat}}/\dot{\epsilon}^*_{\mathrm{lat}} < 1/2$, to be possible where $1/2 \le \dot{\epsilon}_{\mathrm{lat}}/\dot{\epsilon}^*_{\mathrm{lat}} \le 2$, and to be likely where $2 < \dot{\epsilon}_{\mathrm{lat}}/\dot{\epsilon}^*_{\mathrm{lat}}$.

In the supplement, we explore the consequences of using a constant vertical velocity and examine how the results change when we use a vertical velocity that depends linearly on depth. First, we rederive the main theoretical results and show that the linear vertical velocity problem cannot be solved analytically. Thus, we briefly describe an enthalpy-based finite-volume numerical method (Aschwanden et al., 2012; Schoof and Hewitt, 2016; Meyer and Hewitt, 2017) to compute the temperature structure along with the depth and thickness of temperate zones. When the Péclet number is small there is little difference between the constant and linear vertical velocity cases. Finally, we compute analogous plots showing the strain rates and temperate zone thicknesses for regions of the Antarctic Ice Sheet. While the results for the linear vertical velocity case are likely more quantitatively realistic, the constant vertical velocity analytical solutions provide the same spatial patterns and are useful to gain insight into the processes that govern the temperature structure of ice stream shear margins.

Lateral advection of cold ice, which we treat as a depth-averaged value in our model, can be important under some conditions (Suckale et al., 2014; Haseloff et al., 2015). We leave further development of this idea for future work, but note two important considerations related to our results. First, many of the areas where we infer temperate ice are bounded by highs in the bed topography (i.e. margin positions are topographically controlled), which can mitigate the possibility of across-stream advection of cold ice as it is not possible for the margin to migrate. Second, in the present model, there is a one-way thermal coupling between the mechanical and thermal problem, meaning that the strain rate influences the temperature but not vice versa. Consequently, there is no *a priori* reason to expect strain rates to be larger than $\dot{\epsilon}^*_{\mathrm{lat}}$. However, because ice softness A is a function of temperature, there is a thermoviscous feedback that softens and narrows shear margins while simultaneously increasing the shear strain rates. Thus, the fact that shear margins are temperate throughout Antarctica shows that the surface velocity field encodes information about the ice temperature. This confirms our understanding of the thermoviscous feedback mechanism and the importance of temperate ice to outlet glaciers.

Additional effects that are not included in the model could influence the size and distribution of temperate zones predicted by our model but are unlikely to qualitatively alter our results. These effects include the temperature dependence of some material properties (e.g., thermal conductivity) (Cuffey and Paterson, 2010), transient dynamics in outlet glacier and ice stream velocities (Catania et al., 2012; Robel et al., 2013), and cold-air ponding in shear margin crevasses (Harrison et al., 1998). Allowing parameters, such as thermal conductivity, to depend on temperature does not change the structure of the equation, it only makes it more difficult to solve and eliminates the insight gained by the analytical solution. We choose a steady state model in order to understand the locations where temperate ice could exist under steady forcing, rather than to ascertain the exact size of all temperate zones in Antarctica, which would require a precise history of transient ice velocity dynamics and prior margin migration rates. Cold-air ponding will affect the temperature near the surface and increase the amount of sensible heat required by shearing to generate a temperate zone. We simulated the influence of cold-air ponding by reducing the surface temperature (shown in Fig. 3b) everywhere by $15\,^{\circ}\mathrm{C}$ and rerunning the model. Colder surface temperatures reduce the Brinkman numbers but the results, which are given in the supplement (Figs. S7 and S8), are qualitatively similar to those shown in the main text. We can understand the similarity between the results for mean-annual and cold-air ponding cases by considering that colder surface temperatures only change the Brinkman number, which causes a translation along the abscissa in the parameter space shown in Fig. 1b. Reducing the surface temperature by $15\,^{\circ}\mathrm{C}$ generally changes $\mathtt{Br}$ by less than a factor of 2, which Fig. 1b shows to be inadequate to extinguish a reasonably thick temperate zone.

In closing, we note that a broader application of this work is to augment large-scale ice-flow models and coupled climate-ice-sheet models by contributing a computationally inexpensive method for estimating englacial temperature profiles, i.e. Equation (13). When coupled with a model for ice softness A as a function of temperature (cf. Cuffey and Paterson, 2010), this approach would provide estimates of ice softness in shear margins. These estimates of A could be efficiently updated as flow speeds and climate conditions change in transient model runs (Joughin et al., 2014; DeConto and Pollard, 2016) and would make viable initial guesses for spatially varying A for use with inverse methods aimed at inferring basal conditions and ice rheology (Joughin et al., 2004; Gudmundsson et al., 2012; Morlighem et al., 2013). This would enable large-scale models to represent the thermoviscous feedback, a potentially important mechanism in ice-sheet evolution.

5. Conclusions

Shear margins of fast flowing glaciers and ice streams are a primary source of resistance to ice flow. Shear stress in the margins is a function of the rheology of ice, which depends on the ice temperature. As ice deforms, work is converted to heat that warms, and thereby softens, the ice. This thermomechanical coupling leads to a thermoviscous feedback that can generate temperate ice in shear zones that are surrounded by relatively cold ice. To understand the spatial distribution and thickness of shear-induced temperate zones in Antarctica, we derive an analytical thermomechanical model that accounts for advection, diffusion, and shear heating. Our model defines the critical shear strain rate at which a temperate zone might initiate, and allows for predictions of the thickness of temperate zones. Using recent observations and outputs from a regional climate model, we show that zones of temperate ice could exist in the shear margins of numerous outlet glaciers and ice streams in the Antarctic Ice Sheet. Highlighting six regions of interest, we show that some glaciers with zones of temperate ice exist in areas where the vertical advection of cold ice from the surface is low due to low surface accumulation rates. Glaciers in the Amundsen Sea Embayment, West Antarctica, are among the few areas where extreme strain rates may overcome rapid downward vertical advection of cold ice to possibly produce zones of temperate ice. In this regard, Pine Island Glacier, West Antarctica, stands out as potentially supporting thick zones of temperate ice, in the absence of lateral advection of cold ice. In glaciers where our model predicts thick temperate zones immediately upstream of the grounding line, shear margins extend to great distances (>100 km) onto the floating ice shelf. We hypothesize that this is due to the downstream advection of warm, soft ice onto the ice shelf. As a result, the development of temperate ice upstream of the grounding line might help determine the structural integrity of the ice shelf and to modulate the ability of the ice shelf to buttress the glacier, thereby generating the potential for ice-sheet retreat due to thermoviscous feedbacks.

Acknowledgements

We wish to thank Jim Rice, Alan Rempel, and Jenny Suckale for insightful discussions. We are grateful to the scientific editor Bruce Buffett as well as Kurt Cuffey and an anonymous reviewer for suggesting improvements to this manuscript. We also thank J.M. van Wessen for providing surface mass balance and temperature from RACMO2.3 and Alex Gardner for providing the Landsat-derived surface velocity fields. We are grateful for the support of the NSF Graduate Research Fellowship award DGE1144152 and a David Crighton Fellowship to CRM and the NSF Earth Sciences Postdoctoral Fellowship award EAR1452587 to BMM.

Appendix A. Supplementary material

Supplementary material related to this article can be found online at https://doi.org/10.1016/j.epsl.2018.06.028.

References

Aschwanden, A., Bueler, E., Khroulev, C., Blatter, H., 2012. An enthalpy formulation for glaciers and ice sheets. J. Glaciol. 58, 441–457. https://doi.org/10.3189/2012JoG11J088.

Catania, G., Hulbe, C., Conway, H., Scambos, T.A., Raymond, C.F., 2012. Variability in the mass flux of the Ross ice streams, West Antarctica, over the last millennium. J. Glaciol. 58, 741–752. https://doi.org/10.3189/2012JoG11J219.

Clarke, G.K.C., Nitsan, U., Paterson, W.S.B., 1977. Strain heating and creep instability in glaciers and ice sheets. Rev. Geophys. 15, 235–247. https://doi.org/10.1029/RG015i002p00235.

Cuffey, K.M., Paterson, W.S.B., 2010. The Physics of Glaciers, fourth edition. ISBN 9780123694614. Elsevier.

DeConto, R.M., Pollard, D., 2016. Contribution of Antarctica to past and future sea-level rise. Nature 531, 591–597. https://doi.org/10.1038/nature17145.

Echelmeyer, K., Harrison, W., 1999. Ongoing margin migration of Ice Stream B, Antarctica. J. Glaciol. 45, 361–369. https://doi.org/10.3189/002214399793377059.

Echelmeyer, K.A., Harrison, W.D., Larsen, C., Mitchell, J.E., 1994. The role of the margins in the dynamics of an active ice stream. J. Glaciol. 40, 527–538. https://doi.org/10.3198/1994JoG40-136-527-538.

Elsworth, C.W., Suckale, J., 2016. Rapid ice flow rearrangement induced by subglacial drainage in West Antarctica. Geophys. Res. Lett. 43, 697–707. https://doi.org/10.1002/2016GL070430.

Fowler, A.C., Johnson, C., 1996. Ice-sheet surging and ice-stream formation. Ann. Glaciol. 23, 68–73. https://doi.org/10.3189/1996AoG23-68-73.

Fretwell, P., Pritchard, H.D., Vaughan, D.G., Bamber, J.L., Barrand, N.E., Bell, R., Bianchi, C., Bingham, R.G., Blankenship, D.D., Casassa, G., et al., 2013. Bedmap2: improved ice bed, surface and thickness datasets for Antarctica. Cryosphere 7. https://doi.org/10.5194/tc-7-375-2013.

Gardner, A.S., Moholdt, G., Scambos, T., Fahnstock, M., Ligtenberg, S., van den Broeke, M., Nilsson, J., 2018. Increased West Antarctic and unchanged East Antarctic ice discharge over the last 7 years. Cryosphere 12, 521–547. https://doi.org/10.5194/tc-12-521-2018.

Gudmundsson, G.H., Krug, J., Durand, G., Favier, L., Gagliardini, O., 2012. The stability of grounding lines on retrograde slopes. Cryosphere 6, 1497–1505. https://doi.org/10.5194/tc-6-1497-2012.

Harrison, W.D., Echelmeyer, K.A., Larsen, C.F., 1998. Measurement of temperature in a margin of Ice Stream B, Antarctica: implications for margin migration and lateral drag. J. Glaciol. 44, 615–624. https://doi.org/10.3189/S0022143000002112.

Haseloff, M., Schoof, C., Gagliardini, O., 2015. A boundary layer model for ice stream margins. J. Fluid Mech. 781, 353–387. https://doi.org/10.1017/jfm.2015.503.

Hewitt, I.J., Schoof, C., 2017. Models for polythermal ice sheets and glaciers. Cryosphere 11, 541–551. https://doi.org/10.5194/tc-11-541-2017.

Hindmarsh, R.C.A., 2004. Thermoviscous stability of ice-sheet flows. J. Fluid Mech. 502, 17–40. https://doi.org/10.1017/S0022112003007390.

Hindmarsh, R.C.A., 2009. Consistent generation of ice-streams via thermo-viscous instabilities modulated by membrane stresses. Geophys. Res. Lett. 36, L06502. https://doi.org/10.1029/2008GL036877.

Howell, P.D., Kozyreff, G., Ockendon, J.R., 2008. Applied Solid Mechanics. Cambridge University Press.

Hutter, K., 1983. Theoretical Glaciology. D. Reidel Publishing Co./Terra Scientific Publishing Co., Tokyo.

Jacka, T.H., Budd, W.F., 1989. Isotropic and anisotropic flow relations for ice dynamics. Ann. Glaciol. 12, 81–84. https://doi.org/10.3189/1989AoG12-1-81-84.

Jackson, M., Kamb, B., 1997. The marginal shear stress of Ice Stream B, West Antarctica. J. Glaciol. 43, 415–426. https://doi.org/10.3198/1997JoG43-145-415-426.

Jacobson, H.P., Raymond, C.F., 1998. Thermal effects on the location of ice stream margins. J. Geophys. Res. 103, 12111–12122. https://doi.org/10.1029/98JB00574.

Jezek, K.C., Curlander, J.C., Carsey, F., Wales, C., Barry, R.G., 2013. RAMP AMM-1 SAR Image Mosaic of Antarctica. Version 2. Technical Report. National Snow and Ice Data Center, Boulder, Colorado, USA.

Johnson, K.L., 1987. Contact Mechanics. Cambridge University Press.

Joughin, I., MacAyeal, D.R., Tulaczyk, S., 2004. Basal shear stress of the Ross ice streams from control method inversions. J. Geophys. Res. 109, 1–20. https://doi.org/10.1029/2003JB002960.

Joughin, I., Smith, B.E., Medley, B., 2014. Marine ice sheet collapse potentially under way for the Thwaites Glacier Basin, West Antarctica. Science 344, 735–738. https://doi.org/10.1126/science.1249055.

Kamb, B., 2001. Basal zone of the West Antarctic ice streams and its role in lubrication of their rapid motion. In: Alley, R.B., Bindschadler, R.A. (Eds.), The West Antarctic Ice Sheet: Behavior and Environment, vol. 77. AGU, Washington, DC, pp. 157–199.

Kyrke-Smith, T.M., Katz, R.F., Fowler, A.C., 2013. Subglacial hydrology and the formation of ice streams. Proc. R. Soc. Lond. Ser. A 470. https://doi.org/10.1098/rspa.2013.0494.

Meyer, C.R., Fernandes, M.C., Creyts, T.T., Rice, J.R., 2016. Effects of ice deformation on Röthlisberger channels and implications for transitions in subglacial hydrology. J. Glaciol. 62, 750–762. https://doi.org/10.1017/jog.2016.65.

Meyer, C.R., Hewitt, I.J., 2017. A continuum model for meltwater flow through compacting snow. Cryosphere 11, 2799–2813. https://doi.org/10.5194/tc-11-2799-2017.

Meyer, C.R., Hutchinson, J.W., Rice, J.R., 2017. The path-independent M integral implies the creep closure of englacial and subglacial channels. J. Appl. Mech. 84, 011006. https://doi.org/10.1115/1.4034828.

Minchew, B.M., Meyer, C.R., Gudmundsson, G.H., Robel, A.A., Simons, M., 2018. Processes controlling the downstream evolution of ice rheology in glacier shear margins: case study on Rutford Ice Stream, West Antarctica. J. Glaciol. https://doi.org/10.1017/jog.2018.47. In press.

Morlighem, M., Seroussi, H., Larour, E., Rignot, E., 2013. Inversion of basal friction in Antarctica using exact and incomplete adjoints of a higher-order model. J. Geophys. Res. 118, 1746–1753. https://doi.org/10.1002/jgrf.20125.

Mouginot, J., Rignot, E., Scheuchl, B., Millan, R., 2017. Comprehensive annual ice sheet velocity mapping using Landsat-8, Sentinel-1, and RADARSAT-2 data. Remote Sens. 9, 364. https://doi.org/10.3390/rs9040364.

Mouginot, J., Scheuchl, B., Rignot, E., 2012. Mapping of ice motion in Antarctica using synthetic-aperture radar data. Remote Sens. 4, 2753–2767. https://doi.org/10.3390/rs4092753.

Perol, T., Rice, J.R., 2011. Control of the width of West Antarctic ice streams by internal melting in the ice sheet near the margins. Abstract C11B-0677 presented at 2011 Fall Meeting, AGU, San Francisco, Calif., 5–9 Dec.

Perol, T., Rice, J.R., 2015. Shear heating and weakening of the margins of West Antarctic ice streams. Geophys. Res. Lett. 42, 3406–3413. https://doi.org/10.1002/2015gl063638.

Perol, T., Rice, J.R., Platt, J.D., Suckale, J., 2015. Subglacial hydrology and ice stream margin locations. J. Geophys. Res. 120, 1–17. https://doi.org/10.1002/2015jf003542.
Raymond, C., 1996. Shear margins in glaciers and ice sheets. J. Glaciol. 42, 90–102. https://doi.org/10.3198/1996JoG42-140-90-102.
Rignot, E., Mouginot, J., Scheuchl, B., 2011. Ice flow of the Antarctic ice sheet. Science 333, 1427–1430. https://doi.org/10.1126/science.1208336.
Robel, A.A., DeGiuli, E., Schoof, C., Tziperman, E., 2013. Dynamics of ice stream temporal variability: modes, scales, and hysteresis. J. Geophys. Res. 118, 925–936. https://doi.org/10.1002/jgrf.20072.
Schoof, C., 2004. On the mechanics of ice-stream shear margins. J. Glaciol. 50, 208–218. https://doi.org/10.3189/172756504781830024.
Schoof, C., 2012. Thermally driven migration of ice-stream shear margins. J. Fluid Mech. 712, 552–578. https://doi.org/10.1017/jfm.2012.438.
Schoof, C., Hewitt, I., 2013. Ice-sheet dynamics. Annu. Rev. Fluid Mech. 45, 217–239. https://doi.org/10.1146/annurev-fluid-011212-140632.
Schoof, C., Hewitt, I.J., 2016. A model for polythermal ice incorporating gravity-driven moisture transport. J. Fluid Mech. 797, 504–535. https://doi.org/10.1017/jfm.2016.251.
Suckale, J., Platt, J.D., Perol, T., Rice, J.R., 2014. Deformation-induced melting in the margins of the West Antarctic ice streams. J. Geophys. Res. 119, 1004–1025. https://doi.org/10.1002/2013jf003008.
Tulaczyk, S., Kamb, B., Engelhardt, H.F., 2000. Basal mechanics of Ice Stream B, West Antarctica: 2. Undrained plastic bed model. J. Geophys. Res. 105, 483–494. https://doi.org/10.1029/1999jb900328.
Van der Veen, C.J., 1998. Fracture mechanics approach to penetration of bottom crevasses on glaciers. Cold Reg. Sci. Technol. 27, 213–223.
van Wessem, J.M., Reijmer, C.H., Morlighem, M., Mouginot, J., Rignot, E., Medley, B., Joughin, I., Wouters, B., Depoorter, M.A., Bamber, J.L., et al., 2014. Improved representation of East Antarctic surface mass balance in a regional atmospheric climate model. J. Glaciol. 60, 761–770. https://doi.org/10.3189/2014JoG14J051.
Worster, M.G., 2000. Solidification of fluids. In: Batchelor, G.K., Moffatt, H.K., Worster, M.G. (Eds.), Perspectives in Fluid Dynamics. Cambridge University Press, pp. 393–444 (Chapter 8).